Bioresource Technology 343 (2022) 126098

Contents lists available at ScienceDirect

Bioresource Technology

journal homepage: www.elsevier.com/locate/biortech

Microbial community assembly and dynamics in Granular, Fixed-Biofilm and planktonic microbiomes valorizing Long-Chain fatty acids at 20 °C

Suniti Singh [a,b,c], Johanna M. Rinta-Kanto [a], Piet N.L. Lens [a,b], Marika Kokko [a], Jukka Rintala [a], Vincent O'Flaherty [c], Umer Zeeshan Ijaz [d,*], Gavin Collins [c,d]

[a] Faculty of Engineering and Natural Sciences, Tampere University, P.O. Box 541, FI-33104 Tampere University, Finland
[b] UNESCO-IHE, Institute for Water Education, Westvest 7, 2611AX Delft, the Netherlands
[c] School of Chemical and Biological Sciences, and Ryan Institute, National University of Ireland Galway, University Road, Galway H91 TK33, Ireland
[d] Water and Environment Group, School of Engineering, University of Glasgow, Glasgow G12 8LT, United Kingdom

HIGHLIGHTS

- Granular, biofilm and planktonic assemblages developed from the same seed reservoir.
- Three assemblages forming metacommunity differed in diversity and composition.
- Multiple null models applied to quantify deterministic and stochastic mechanisms.
- Dominant, active role of acetoclastic *Methanosaeta* confirmed in granules and biofilm.
- Dynamic, non-core-microbiome taxa correlated with environmental variables.

GRAPHICAL ABSTRACT

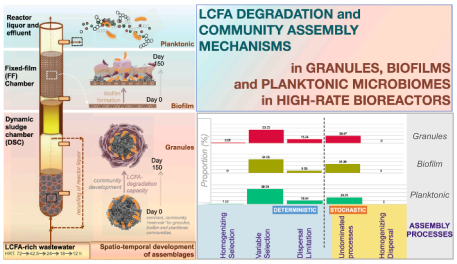

ARTICLE INFO

Keywords:
Fats, oils, and grease (FOG)
Low-temperature anaerobic digestion
Methanogenesis
Microbial community assembly
Null modelling

ABSTRACT

Distinct microbial assemblages evolve in anaerobic digestion (AD) reactors to drive sequential conversions of organics to methane. The spatio-temporal development of three such assemblages (granules, biofilms, planktonic) derived from the same inoculum was studied in replicated bioreactors treating long-chain fatty acids (LCFA)-rich wastewater at 20 °C at hydraulic retention times (HRTs) of 12–72 h. We found granular, biofilm and planktonic assemblages differentiated by diversity, structure, and assembly mechanisms; demonstrating a spatial compartmentalisation of the microbiomes from the initial community reservoir. Our analysis linked abundant *Methanosaeta* and *Syntrophaceae*-affiliated taxa (*Syntrophus* and *uncultured*) to their putative, active roles in syntrophic LCFA bioconversion. LCFA loading rates (stearate, palmitate), and HRT, were significant drivers shaping microbial community dynamics and assembly. This study of the archaea and syntrophic bacteria actively valorising LCFAs at short HRTs and 20 °C will help uncover the microbiology underpinning anaerobic bioconversions of fats, oil and grease.

* Corresponding author.
E-mail address: umer.ijaz@glasgow.ac.uk (U.Z. Ijaz).

https://doi.org/10.1016/j.biortech.2021.126098
Received 3 August 2021; Received in revised form 3 October 2021; Accepted 5 October 2021
Available online 7 October 2021

1. Introduction

Microbial consortia have been exploited for numerous biotechnological applications, such as for valorizing wastewaters, principally because mixed-species systems allow for easier management and provide more diverse applications than pure-culture set-ups (McCarty and Ledesma-Amaro, 2019). The anaerobic digestion (AD) process, in particular, relies on the concerted activity of multiple microbial trophic groups to sequentially drive the bioconversion of organic matter to methane and CO_2 in various assemblage modes – granular, biofilm or planktonic – and bioreactor configurations (Abdelgadir et al., 2014). The composition of the underlying methanogenic consortia responds to environmental and process selection pressures (Nemergut et al., 2013). Microbial taxa variously interact in forming community assemblages that are structured as biofilm slimes, flocs, granules and other aggregates, or, as planktonic communities (Aqeel et al., 2019). Thus, AD assemblages harbouring multiple trophic-level interactions serve as suitable communities to evaluate microbial community dynamics and assembly.

Unveiling microbial assembly mechanisms offers unprecedented insights into engineered bioconversion systems, such as AD bioreactors (Ferguson et al., 2018). Factors such as inoculum composition (Li et al., 2019; Singh et al., 2019a), substrate composition and loading (Braz et al., 2019; Chen et al., 2019), operational duration (Lucas et al., 2015; Vanwonterghem et al., 2014), and process temperature (Heidrich et al., 2018), were shown as strong drivers of microbial community assembly in various AD systems when operated at hydraulic retention times (HRTs) longer than 10 d. However, shorter HRTs (<3 d) are sought to economize the anaerobic wastewater treatment process. Under such conditions, stochastic community assembly may be promoted due to random changes from immigration, drift or dispersal of microbial taxa (Nemergut et al., 2013; Stegen et al., 2012). Alternatively, short HRTs may promote environmental filtering due to the selection of taxa with unique survival potential (Stegen et al., 2012; Zhou, 2017). Treatment of organics, including inhibitory compounds at low (sub-mesophilic) temperatures is also desirable in AD systems to improve the net energy yield (Petropoulos et al., 2019), but such conditions are regarded as challenging for optimal functioning of AD consortia. Operational conditions, including HRTs, the presence of inhibitory compounds, and operating temperatures, are likely drivers of microbial community assembly in methanogenic consortia. A mechanistic understanding of the concerted effects of these challenging growth conditions on the microbial community dynamics and assembly of methanogenic consortia will aid in further widening the applications of AD for waste bioconversion and valorisation.

A growing body of literature has characterized assembly and succession of microbial communities in granules (Liébana et al., 2019), biofilms (Xu et al., 2019) and planktonic assemblages (Xu et al., 2020) obtained from engineered microcosms, including more recently from AD bioreactors (Trego et al., 2021). However, AD bioreactors may rely on distinct assemblage types to perform specific roles across reactor compartments (e.g., in hybrid bioreactors containing both granular and fixed-film biofilm; Singh et al., 2020). Thus, a systematic inference of the selective environmental pressures on the development of distinct assemblages from a common, seed community reservoir in AD bioreactors is needed to comprehend their comparative roles and assembly mechanisms.

The objective of this study was to characterize three distinct microbial assemblages (granules, biofilm, and planktonic communities) that were sampled from replicated bioreactors inoculated with one community reservoir of anaerobic sludge. The assemblages were developed in novel, two-compartment bioreactors treating long-chain fatty acids (LCFA)-rich wastewater at low HRTs (72–12 h) at 20 °C, which we previously evaluated and reported (Singh et al., 2020). The temporal variations in active microbiomes from each of the assemblages were studied to evaluate the effect of environmental variables on microbial community dynamics (diversity, composition, and core and dynamic taxa). We applied multiple null model approaches to study community assembly, and to quantify the relative contribution of assembly processes involved in structuring the three assemblages.

2. Materials and methods

2.1. Sample collection

Microbial samples were collected from three, identical anaerobic dynamic sludge chamber-fixed film (DSC-FF) bioreactors, which were operated in parallel to treat mixed-LCFA-rich synthetic dairy wastewater at 20 °C for 150 d as described previously (Singh et al., 2020). Granules from the sludge-bed layer (the DSC), the biofilm (the FF, which was grown on pumice stones) and the planktonic community from effluent samples were collected from different operating phases at the applied HRTs (72, 42.5, 24, 18, 12 h) corresponding to days 8, 24, 58, 100 and 148. The anaerobic sludge used as the inoculum was also sampled. Pumice stones were aseptically collected from the FF section, and, sonicated in an ultrasonic water bath (PUL-125 ultrasonic bath, Kerry Ultrasonics, England) with an output power of 150 W at 28 kHz for 5 min at 20 °C with 10 mL of phosphate buffer saline (pH 7.2) to dislodge microbial cells from the attached biofilm. The supernatant from biofilm, and the effluent samples (25 mL), were each centrifuged at 8,000 rpm for 10 min (8,470 × *g*) at 4 °C to harvest cells. The resultant pellets, along with the granules and the inoculum samples, were flash-frozen in liquid nitrogen immediately upon collection and stored at −80 °C.

2.2. Nucleic acids extraction and 16S rRNA gene amplicon sequencing

The microbial samples were thawed on ice, and the nucleic acids (DNA and RNA) were extracted using the phenol chloroform method, followed by quantification of DNA and RNA concentrations using a Qubit fluorometer (Life Technologies), and evaluation of DNA purity using a Nanodrop (NanoDrop Technologies, Wilmington, USA) and gel electrophoresis (Singh, 2019). Next, DNase treatment was performed to remove DNA using Invitrogen Turbo-DNase kit (Thermo Fisher, USA) by following the recommended procedure, and the DNA-free samples consisting of RNA were converted to cDNA using M−MuLV Reverse Transcriptase kit (New England BioLabs, USA) according to the instructions provided by the supplier. PCR amplification of the V4 region of the 16S rRNA gene was performed on cDNA transcripts with the universal primers 515f and 806r (Caporaso et al., 2011), with the sequencing of the active microbiomes on the Illumina MiSeq platform using 2x300 bp paired-end run. Biofilm and effluent samples obtained from 72 h HRT were not sequenced because extractions yielded inadequate quantities of cDNA. The 16S rRNA sequences used to support the findings of this study have been deposited in the NCBI Sequence Read Archive under bioproject accession PRJNA657615.

2.3. Bioinformatics and statistical analysis

The sequence data was analyzed using Quantitative Insights Into Microbial Ecology (QIIME v1.9, and QIIME v2) pipeline (Bolyen et al., 2019; Caporaso et al., 2010). The paired-end reads were joined using a fastq-join method with a min overlap of 50 bp and a perc_max_diff of 15%, after which quality filtering was performed using the split_libraries_fastq.py script in QIIME. The sequences were clustered into operational taxonomic units (OTUs) using the open-reference OTU picking with uclust using default settings. It should be noted that chimeric sequences were identified using ChimeraSlayer and the final OTU table was generated from the nonchimeric sequences following standard recommendations in QIIME. QIIME2 was then utilised to assign taxonomy using the SILVA SSU Ref NR database release v.132 as well as to generate the rooted phylogenetic tree after alignment of the OTU sequences.

Statistical analyses were performed in R using all of the OTUs (data generated as above) as well as the meta data associated with the study. The details of these methods are given in authors' recent publications (Nikolova et al., 2021; Trego et al., 2021). For alpha diversity, we calculated: (i) rarefied richness – This gives the estimated number of species in a rarefied sample (to minimum library size); (ii) Pielou's evenness – This gives the diversity values from 0 (no evenness) to 1 (complete evenness). The figures were then supplemented with p-values from Analysis of Variance (ANOVA) where significant. Furthermore, we utilized phylogenetic alpha diversity measures such as (i) nearest taxa index (NTI), which, is a measure of mean pairwise phylogenetic distance at local level and quantifies tip-level divergences (putting more emphasis on terminal clades and is akin to "local" clustering) in phylogeny; and (ii) net relatedness index (NRI), which, is a measure of mean pairwise phylogenetic distance of all the taxa in a sample, relative to phylogeny of an appropriate species pool and quantifies overall clustering of taxa on a tree. Briefly, these methods record original phylogenetic distances in a phylogenetic tree, and then generate 1000 randomizations of the phylogenetic tree (whilst keeping richness preserved) to calculate the phylogenetic distances on these distributions. Afterwards, the mean and standard deviation of these distances obtained from randomization procedure are used in a method called "statistical effect size" for comparison against the original distances to give NRI/NTI estimates. The values of NRI/NTI hold importance as they can be used to discern an underlying ecological mechanism. For a single community, NTI values $> +2$ suggest environmental filtering (phylogenetic clustering), and values $<$ -2 indicate competitive exclusion (phylogenetic overdispersion) among species as the driver of community structure (Stegen et al., 2012). Although both NRI and NTI use similar thresholding cut off, NTI is typically preferred over NRI for ecological interpretation because of the presence of phylogenetic signal across short phylogenetic distances (Wang et al., 2013).

For beta diversity, the dissimilarity in species community composition between pairwise comparisons of bacterial communities were represented in Principal Coordinate Analysis (PCoA) ordination plots by calculating three different dissimilarity measures between the samples: (i) *Bray Curtis distance* that only considers the species abundance of samples; (ii) *Unweighted Unifrac distance* that is based on the proportion of phylogenetic tree shared between the samples by calculating branch lengths, and (iii) *Weighted Unifrac distance* which is similar to (ii) but weights the branch lengths by species abundance counts. In all three cases, the resulting distance values are normalized between 0 (similar) and 1 (dissimilar) for any pair of samples, and when used in an ordination plot (PCoA), they provide visual cues on how similar the samples are. The PCoA plots were further supplemented with ellipses representing the standard errors of the (weighted) averages of the sample values on PCoA plot, and this is plotted for each sample group (assemblage type or HRT).

We then used the core microbiome analysis by selecting taxa that have a minimum prevalence of 85% across all the samples. Furthermore, two dimensional plot at varying detection threshold (abundances) was obtained for these selected taxa (Lahti et al., 2019). To find the taxa that are important for variance in microbial community, a subset analysis was performed to reduce the OTU table to the minimum set of representative OTUs that roughly preserved the same beta diversity between the samples as the entire OTU table. The procedure uses Bray Curtis distance to record all the pairwise distances between the samples using all the observed OTUs. These recorded distances were then correlated with the distances obtained from different permutations of the original table (considering the top 2000 abundant OTUs) in an iterative manner. Using the top subsets, we then performed PERMANOVA against all sources of variation (sample grouped by assemblage types or HRT) to see if these subsets are significant. To reduce the associated meta data (physico-chemical parameters) to meaningful parameters, Redundancy analysis (RDA) on the Hellinger-transformed sequence data with forward selection (based on 999 permutations, variables retained at $p <$ 0.05) was performed to select for environmental variables most strongly associated with the variance of the observed microbial communities. Finally, correlation analysis was performed to measure the strength of association between representative OTUs (obtained from subset analysis) and the selected environmental variables, using Kendall correlation. The p-values were then adjusted for multiple comparisons using Benjamini and Hochberg procedure to give significant associations.

2.4. Null model quantification of microbial assembly mechanisms and ecological processes

Different null modeling approaches with different analytical formulations were performed to achieve a general consensus on community assembly trends, and to mask out any biases associated with the methods. First, ecological stochasticity in community assembly was calculated based on beta diversity using Normalized Stochasticity ratio (NST) with various distance measures (incidence-based: Jaccard, Kulczynski and abundance-based: Ruzcika, Kulczynski) in R using the NST package with 50% as the boundary point between more deterministic ($<$50%) and more stochastic ($>$50%) assembly (Ning et al., 2019). For the calculations, the taxa occurrence frequency and the sample richness were constrained as proportional (P) or fixed (F) in the combinations PF or PP, and 1000 randomizations were performed for each model. Statistical significance was computed based on permutational multivariate ANOVA (PANOVA). NST values rely on the underlying beta diversity distance metrics used. Some of these distance metrics do not consider phylogeny in calculating the dissimilarities and may not be appropriate to discern the ecological phenomena. Secondly, some of the beta diversity distance metrics do not have a fixed upper limit or clearly defined similarity measure, and as a result a further standardization procedure is required before using NST. Nonetheless, these limitations in NST usage were avoided by using the recommended distance measures where a simulated community with known stochasticity values was evaluated and achieved high accuracy and precision (Ning et al., 2019).

Next, we used an alternative approach utilizing Quantitative Process Estimates (QPE)(Vass et al., 2020) to further explore the prevailing ecological niches, breaking down the community assembly mechanisms into five ecological processes, namely, 'homogenizing selection', 'variable selection', 'dispersal limitation', 'homogenizing dispersal', and 'undominated stochastic processes'. This is a preferred approach as it also utilises the phylogenetic tree and describes microbial community assembly processes in terms of *selection* (variable or homogenous), *dispersal* (dispersal limitation, or homogenising dispersal) or 'undominated' mechanisms (Stegen et al., 2015; Vellend, 2010). Variable selection leads to several ecological niches due to different selective environmental conditions, whilst homogenous selection holds when stable environmental conditions result in consistent selective pressure. Dispersal processes refer to the movement of microbes throughout the space. High rates of dispersal result in similar communities, referred to as homogenising dispersal. Conversely, dispersal limitation increases differences in community composition resulting in more dissimilar communities and occurs when low dispersal rates result in a high community turnover. Generally, dispersal limitation drives ecological drift, and is considered a stochastic assembly process.

To obtain the above estimates, using the OTU abundance table and the phylogeny, deviation from the observed βMNTD (β-mean-nearest-taxon-distance) and the mean of the null distribution was evaluated using βNTI (β-nearest-taxon-index) for each pair of samples (n) in a sample group (assemblage type or HRT) recording n(n-1)/2 comparisons. When the observed value of βMNTD deviated significantly from the null expectation, the community was assembled by variable (βNTI $>+2$) or homogenous (βNTI < -2) selection processes, and these were obtained as the proportion of all pairwise comparisons where the thresholds were satisfied. If the difference was not significant, the observed differences in phylogenetic composition were considered to be the result of dispersal mechanisms enabling ecological drift. These were

differentiated using the abundance-based β_{RC} and a Bray-Curtis dissimilarity metric for beta diversity. If the $\beta_{RCbray} > +0.95$, assembly was driven by dispersal limitation coupled with drift; if $\beta_{RCbray} < -0.95$ then homogenising dispersal mechanisms contributed to community assembly; and if β_{RCbray} was between -0.95 and $+0.95$, community turnover was due to undominated mechanisms (i.e., dominated neither by dispersal nor selection processes).

3. Results and discussion

3.1. Microbial diversity patterns in granular, biofilm and planktonic assemblages

Microbial diversity (Fig. 1A,B) in the bioreactors varied with the applied HRT across the three assemblages (granules, biofilm and planktonic communities). Rarefied richness and Pielou's evenness in the granules had not changed by the first sampling (day 8), but both were significantly ($p < 0.01$) reduced when HRT was shortened from 72 to 12 h (Fig. 1A,B). This is in line with the previous studies using anaerobic microcosms, wherein niche specialization was linked to substrate-specific metabolic adaptations in the community (Braz et al., 2019). Meanwhile, in the biofilm, rarefied richness and Pielou's evenness increased significantly ($p < 0.05$) with the growing, *de novo* biofilm and with the changing HRT (Fig. 1A,B). Ultimately (by the time the HRT had been reduced to 12 h), the biofilm community was similarly diverse as, but more even ($p < 0.01$) than in the granules or the planktonic microbiomes.

Phylogenetic alpha diversity analysis further differentiated the three assemblages, since NTI determined significant increase in phylogenetic clustering in the biofilm and planktonic assemblages when the HRT was reduced from 72 to 12 h (NTI > 0, $p < 0.01$) and in granular assemblages when the HRT was reduced from 18 to 12 h (NTI > 0, $p < 0.01$) (Fig. 1D). Environmental filtering (NTI > 0) dominated the three assemblages at the different HRTs; and eventually at 12 h HRT, NTI followed the trend: effluent > granules > biofilm. Thus, NTI values support that deterministic processes (environmental variables) contributed majorly to structuring of the microbial community in the three assemblages during their temporal development. It is noteworthy to mention that NTI is preferred when assessing the presence of significant phylogenetic signal across short phylogenetic distances (Wang et al., 2013), and thus, was considered more useful than NRI due to the lack of substantial trait data in this dataset.

Assemblages when differentiated based on the beta diversity in PCoA plots (Fig. 1E,F,G) revealed an overlap among the granular and biofilm

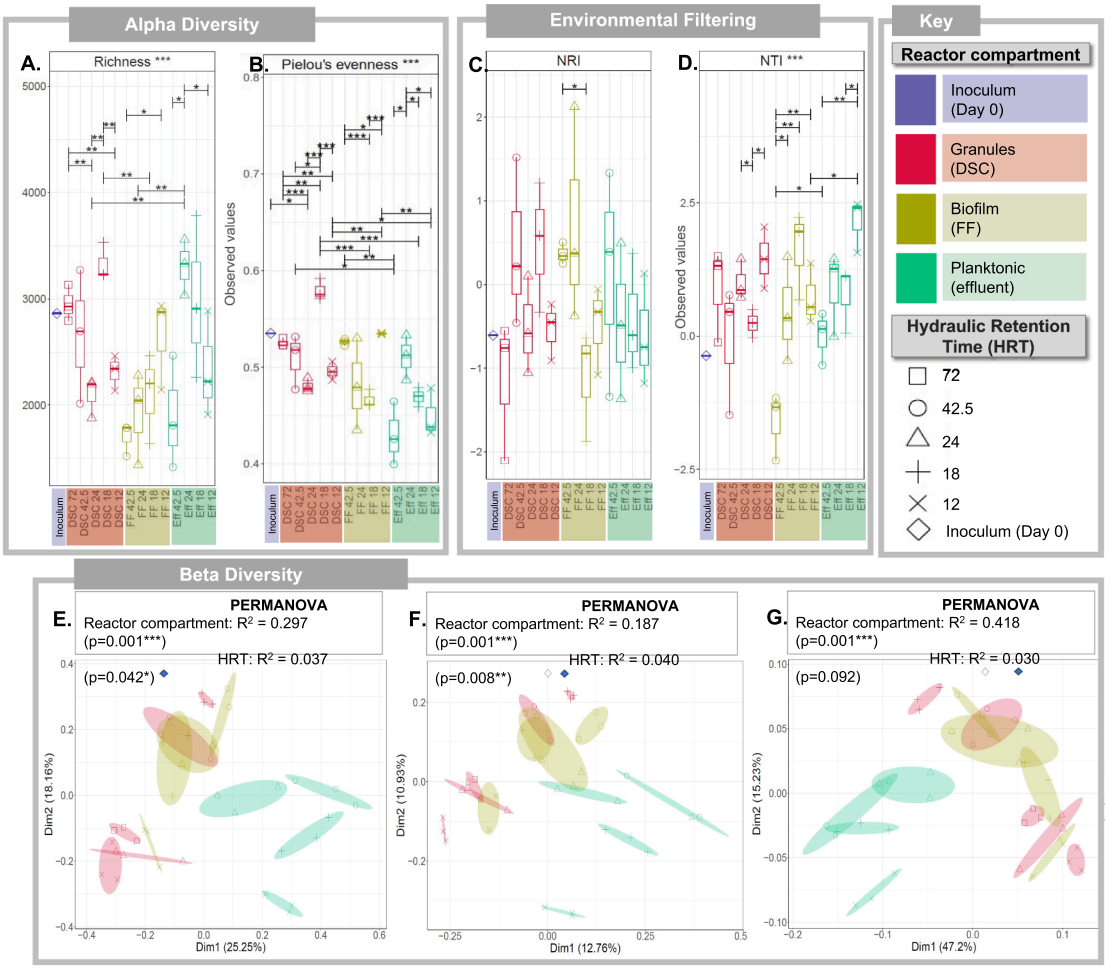

Fig. 1. Diversity in the microbiomes of the inoculum and granular (from DSC), biofilm (from FF) and planktonic (from effluent) assemblages sampled at the different HRTs (72, 42.5, 24, 18 and 12 h). Alpha diversity box plot of the (A) rarefied richness and (B) Pielou's evenness. Environmental filtering box plot of the (C) Net Relatedness Index (NRI) and (D) Nearest Taxa Index (NTI). Beta diversity: PCoA plot calculated using (E) Bray-Curtis distances; (F) unweighted UniFrac distances; and (G) weighted UniFrac distances. Assemblage groups are differentiated by colour, and the ellipses are drawn for each sample group at standard error of ordination points, where arrows mark the direction of change in the community structure between HRTs within assemblage groups that were found to be significant by beta dispersion. PERMANOVA explains significant variability in microbial community structure from different bioreactor compartments and at different HRTs. Lines for panels A, B, C and D connect two sample groups at statistically significant levels indicated by asterisks as * ($p < 0.05$), **($p < 0.01$) or ***($p < 0.001$).

microbiomes at all the HRTs, whereas the planktonic microbiomes clustered distinctly apart. While a majority of the variations between categories was explained by the assemblages (18.7–41.8%) ($p = 0.001$); the HRT further explained 3–4% of the variations between categories (Fig. 1E,F,G).

3.2. Core and dynamic taxa in the granular, biofilm and planktonic assemblages

Ten classes represented 90% of the inoculum community as well as the three assemblages (Fig. 2A), among which 24 genera were highly (>75%) represented (Fig. 2B). These 24 genera were also present in the core microbiome (Fig. 3) of the three assemblages, including the ubiquitous prevalence of *Lactococcus* and uncultured *Syntrophaceae* (prevalence > 90% at reads > 1000). Additionally, *Methanosaeta* and uncultured bacterium *Cloacimonadaceae* were prevalent in the granules and biofilms (Fig. 3), whereas *Pseudomonas* and *Acinetobacter* were more prevalent in the planktonic community (Fig. 3) – demonstrating that differentiation in the core microbiomes was assemblage-specific.

Subset analysis was performed to identify the minimum set of dynamic non-core taxa, namely the representative taxa that statistically explain the observed variances in the community (Table 1). Only five, six and nine taxa represented the variabilities in the beta-diversity of granular, biofilm and planktonic assemblages, respectively (Table 1). This means a small fraction of the sequenced dataset explained 44.8–55.3%, 70–75.8% and 31.3–57.9% of the variation in, respectively, the granules, biofilms, and planktonic microbial community dynamics at the decreasing HRTs in this study. Many of the core taxa (Fig. 3), such as *Methanosaeta*, *Methanobacterium*, uncultured *Syntrophaceae*, *Syntrophus*, *Syntrophobacter* and *Desulfobulbus,* have been previously found to be abundant during LCFA methanization at low ambient temperatures of 10–20 °C (Grabowski et al., 2005; Singh et al., 2019a, 2019b). It is likely that these taxa played an active role at different trophic levels during the successive carbon flow during anaerobic LCFA methanization. During anaerobic treatment, fermentative, and acetogenic, bacteria and the methanogenic archaea are syntrophic partners. The β-oxidizing bacteria require low hydrogen concentrations and form syntrophic partnerships with methanogenic archaea, which scavenge, and maintain low concentrations of, hydrogen. In this study, LCFA methanization was driven by the synergistic relationship wherein acetate and hydrogen produced by the β-oxidizers – *Syntrophus* and *uncultured Syntrophaceae* – were metabolized by the archaea – *Methanobacterium* (hydrogenotrophic methanogen) and *Methanosaeta* (acetoclastic methanogen).

3.3. Quantifying mechanisms structuring the spatial development of assemblages

3.3.1. Assembly mechanisms: Stochastic or deterministic?

We used a suite of null modelling approaches and quantified NST, *βNTI*, *βMNTD* and β_{RCBray} to determine the processes structuring microbial community assembly. The NST indices revealed significant differences in ecological stochasticity amongst the assemblages ($p < 0.001$, PANOVA), irrespective of an evaluation through incidence-based or abundance-based distance matrices, or the constraints imposed on the taxa occurrence frequency and sample richness (Fig. 4A). NST indices

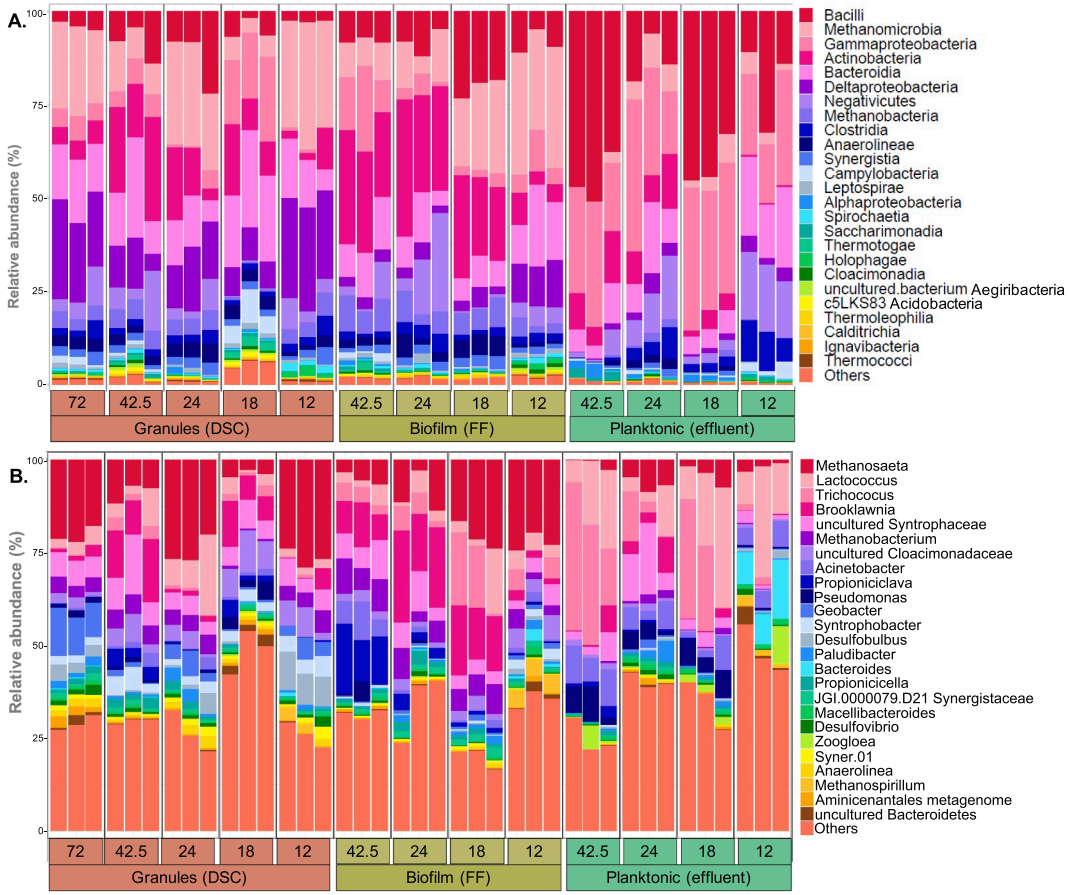

Fig. 2. Barplots of the relative abundance of (A) the 25 most abundant classes, and (B) taxa identified to genus level, found in in the inoculum and the granular (obtained from the DSC), biofilm (obtained from FF), and planktonic (obtained from effluent) assemblages of the triplicate bioreactors R1, R2 and R3, at the HRTs of 72, 42.5, 24, 18 and 12 h. 'Others' are the taxa not included in the 25 most abundant.

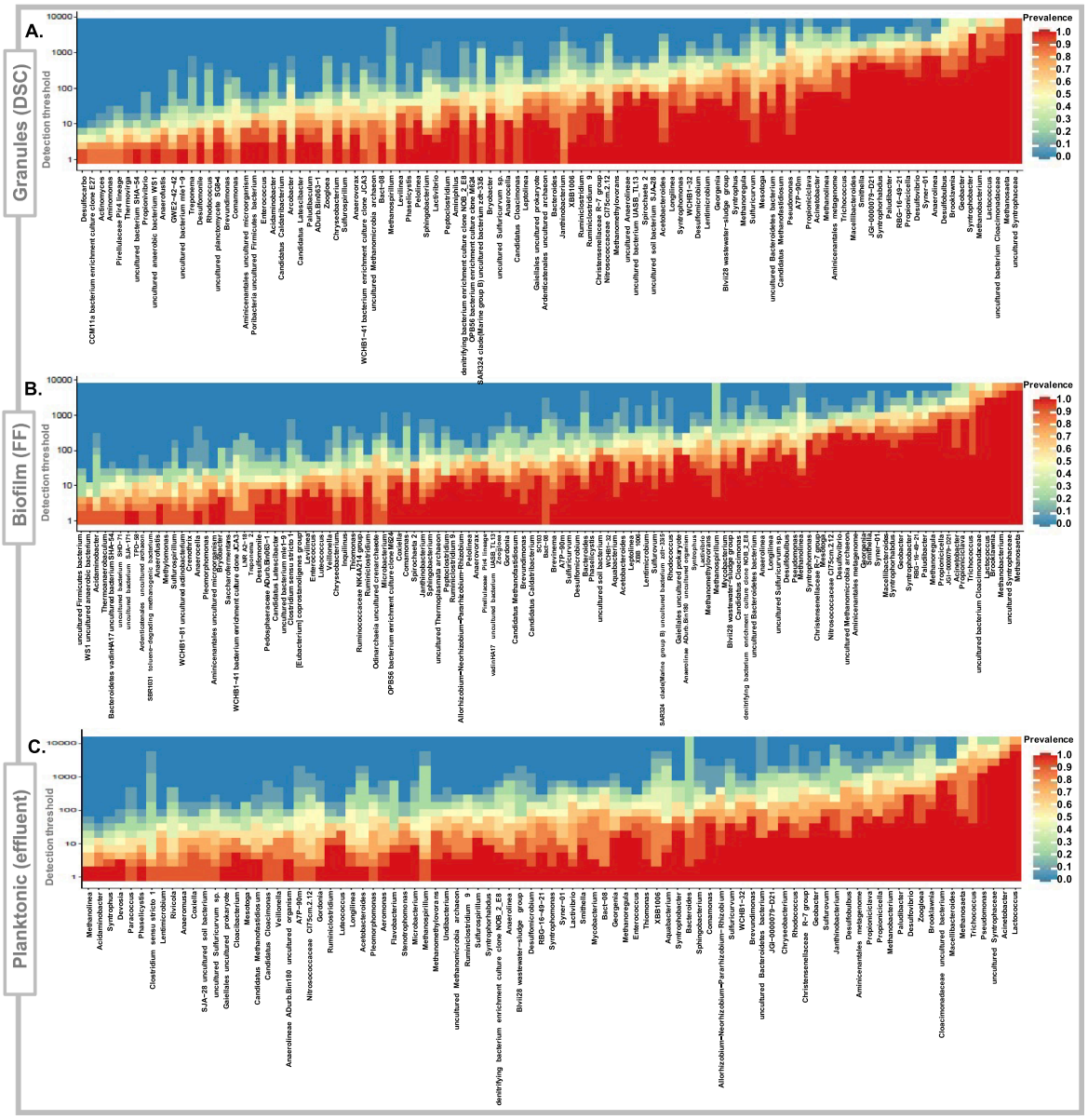

Fig. 3. Highly prevalent taxa in the core microbiomes of (A) granular (from DSC), (B) biofilm (from FF), and (C) planktonic (from effluent) assemblages. Detection thresholds up to 10,000 reads are shown.

were highest for the biofilm and lowest for the effluent (stochasticity trend: biofilm > granules > effluent) (Fig. 4A). QPE analysis revealed that the deterministic processes (55–61%) were higher than the stochastic processes (39–45%) in the assemblages. Trends in total stochasticity ('dispersal limitation', 'homogenizing dispersal', as well as the 'undominated stochastic processes') (Fig. 4B) found using QPE were similar to those found by the NST approach (Fig. 4), i.e, stochasticity followed the trend: biofilm > granules > effluent; and vice-versa for the deterministic causes. These results delineate that granular, biofilm and effluent assemblages have unique signatures, and stochastic and deterministic processes had combined roles in spatially structuring the community assembly in the distinct compartments of DSC-FF bioreactors.

Amongst the deterministic causes, variable selection accounted for the largest proportion of the quantitative process (53–59%) (Fig. 4B), suggesting multiple niches for the selection of species which relied on the prevailing variability in environmental gradients. Dispersal limitation was the highest in the granules (15%), suggesting that among the sludge retention mechanisms (granulation and biofilm formation) in the DSC-FF reactors, granulation constrained dispersal more than biofilm formation. Overall, biofilm had the highest proportion of undominated stochastic processes (36%), and also occupied the highest proportion of all stochastic processes (45%) amongst the assemblages.

We used a comprehensive set of bioinformatics tools and null modelling approaches to quantify the diversity and assembly patterns in the AD assemblages to avoid possible analytical biases. The NST indices showed that both stochastic and deterministic processes shaped the granular, biofilm and planktonic assemblages under 'challenging growth conditions' in the triplicate bioreactors (Fig. 4A). NST is a relatively new measure that estimates stochasticity based on beta diversity measures, employing both incidence-based and abundance-based representations (Ning et al., 2019). Some of the null models also consider phylogenetic clustering as a proxy for the environmental drivers of community assembly. Therefore, looking at the community data with different null models using incidence and abundance matrices and phylogenetic data, our results show consistent assembly patterns (Fig. 4). Moreover, even

Table 1
Correlation of representative taxa (obtained from subset analysis) to the full operational taxonomic unit (OTU) table.

No	Granular assemblage (DSC)	Correlation with full OTU table	PERMANOVA
1	*Rivicola + uncultured bacterium Cloacimonadaceae + uncultured Burkholderiaceae + uncultured bacterium WCHB1-41 + uncultured Syntrophobacterales bacterium Delta_03*	0.951	R2 = 0.553;p = 0.004
2	*Rivicola + uncultured bacterium Cloacimonadaceae + uncultured Burkholderiaceae + uncultured Syntrophobacterales bacterium Delta_03*	0.943	R2 = 0.551;p = 0.003
3	*Rivicola + uncultured bacterium Cloacimonadaceae + uncultured Syntrophobacterales bacterium Delta_03*	0.9301	R2 = 0.551; p = 0.004
4	*Rivicola + uncultured Syntrophobacterales bacterium Delta_03*	0.914	R2 = 0.448; p = 0.067
	Biofilm assemblage (FF)	**Correlation with full OTU table**	**PERMANOVA**
1	*Methanolinea + uncultured bacterium SJA-29 + Geobacter + Christensenellaceae R-7 group + uncultured Veillonellaceae*	0.833	R^2 = 0.75639; p = 0.003
2	*Methanolinea + Methanoregula + uncultured bacterium SJA-29 + Geobacter + Christensenellaceae R-7 group + uncultured Veillonellaceae*	0.828	R^2 = 0.701; p = 0.008
3	*Methanolinea + Geobacter + Christensenellaceae R-7 group + uncultured Veillonellaceae*	0.82	R^2 = 0.758; p = 0.002
4	*Methanolinea + Geobacter + Christensenellaceae R-7 group*	0.809	R^2 = 0.758; p = 0.001
5	*Methanolinea + Christensenellaceae R-7 group*	0.799	R^2 = 0.758; p = 0.002
No	**Planktonic assemblage (effluent)**	**Correlation with full OTU table**	**PERMANOVA**
1	*Rivicola + uncultured bacterium Cloacimonadaceae + uncultured Burkholderiaceae + Methanolinea + Aminicenantales metagenome + uncultured bacterium WCHB1-32 + Syner-01 uncultured bacterium + uncultured Syntrophobacterales bacterium Delta_03 + Azospirillum*	0.951	R^2 = 0.57803; p = 0.001
2	*Rivicola + uncultured bacterium Cloacimonadaceae + uncultured Burkholderiaceae + Methanolinea + Aminicenantales metagenome + uncultured bacterium WCHB1-32 + Syner-01 uncultured bacterium + uncultured Syntrophobacterales bacterium Delta_03*	0.938	R^2 = 0.57854; p = 0.001
3	*Rivicola + uncultured bacterium Cloacimonadaceae + uncultured Burkholderiaceae + Methanolinea + Aminicenantales metagenome + uncultured bacterium WCHB1-32 + Syner-01 uncultured bacterium*	0.927	R^2 = 0.57928; p = 0.001
4	*Rivicola + uncultured bacterium Cloacimonadaceae + uncultured Burkholderiaceae + Methanolinea + Aminicenantales metagenome + uncultured bacterium WCHB1-32*	0.903	R^2 = 0.485; p = 0.021
5	*Rivicola + uncultured bacterium Cloacimonadaceae + uncultured Burkholderiaceae + Aminicenantales metagenome + uncultured bacterium WCHB1-32 + Syner-01 uncultured bacterium*	0.889	R^2 = 0.584; p = 0.001
6	*Rivicola + uncultured bacterium Cloacimonadaceae + uncultured Burkholderiaceae + Aminicenantales metagenome + uncultured bacterium WCHB1-32*	0.867	R^2 = 0.494; p = 0.017
7	*Rivicola + uncultured bacterium Cloacimonadaceae + Aminicenantales metagenome + uncultured bacterium WCHB1-32 + Syner-01 uncultured bacterium*	0.856	R^2 = 0.584; p = 0.004
8	*Rivicola + uncultured bacterium Cloacimonadaceae + Aminicenantales metagenome + uncultured bacterium WCHB1-32*	0.827	R^2 = 0.479; p = 0.012
9	*uncultured bacterium Cloacimonadaceae + Aminicenantales metagenome + uncultured bacterium WCHB1-32 + Syner-01 uncultured bacterium*	0.807	R^2 = 0.521; p = 0.029
10	*uncultured bacterium Cloacimonadaceae + Aminicenantales metagenome + uncultured bacterium WCHB1-32*	0.784	R2 = 0.327; p = 0.297
11	*uncultured bacterium Cloacimonadaceae + Aminicenantales metagenome + Syner-01 uncultured bacterium*	0.762	R^2 = 0.525; p = 0.031
12	*uncultured bacterium Cloacimonadaceae + Aminicenantales metagenome*	0.722	R^2 = 0.313; p = 0.291
13	*uncultured bacterium Cloacimonadaceae + Syner-01 uncultured bacterium*	0.722	R^2 = 0.523; p = 0.022

the observed significant values of phylogenetic alpha diversity measured through NTI at 12 h HRT suggested the dominance of deterministic processes following the trend: effluent > granules > biofilm (Fig. 1D), which was consistent with the trends obtained from the NST and QPE estimations (Fig. 4).

Although conventional evaluations of microbial community assembly provided differentiation between deterministic and stochastic processes (Braz et al., 2019; Lucas et al., 2015), and null modelling approaches have been applied fairly recently for engineered bioreactors (Liébana et al., 2019; Xu et al., 2020; Yuan et al., 2019), we were able for the first time to comprehensively explore microbial community structure and assembly from high-rate, anaerobic LCFA-treating bioreactors using multiple null models.

3.3.2. Environmental variables affecting microbial community assembly

The three assemblages harbouring distinct regional microbial pools were linked hydraulically inside each of the respective bioreactors, and formed a metacommunity in each of the three separate bioreactors. Under short HRTs, microbes with low growth rates will ordinarily be washed out from suspended systems (i.e. those systems without retention on surfaces or in aggregates), leaving rapidly growing microbes as dominant populations (Yuan et al., 2019). Such effects are expected to be even more pronounced at low temperatures because the AD microbiome is considered optimally mesophilic (Pommerville, 2014), yielding diminished growth rates at reduced temperatures (Petropoulos et al., 2019). Moreover, substrate characteristics strongly affect the microbial community structure. For example, LCFAs have a surfactant effect that leads to biofilm thinning and disaggregation of granular sludge (Nikolaeva et al., 2013) and inhibit microbial activity (Astals et al., 2014). Thus, microbes less adept at adhering to biofilm or granular assemblages may be selectively washed-out mobilizing microbes hydraulically within

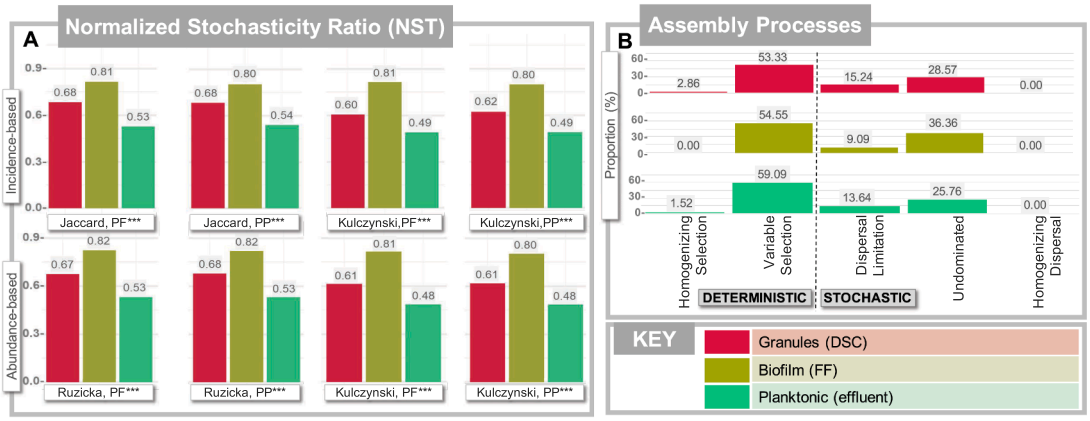

Fig. 4. Estimates of microbial community assembly mechanisms structuring the spatial succession of granular (from DSC), biofilm (from FF) and planktonic (from effluent) assemblages grown from a single microbial community reservoir (inoculum). Spatial variation in (A) normalized stochasticity ratio (NST) indices, calculated as incidence-metrics (Jaccard and Kulczynski distance metrics) and as abundance-metrices (Ruzicka and Kulczynski distance metrices), with PF and PP null models among the granular, biofilm and planktonic assemblages; (B) the proportion of assembly processes by species-sorting (variable or homogeneous selection), dispersal limitation, homogenizing dispersal or undominated stochastic processes among the granular, biofilm and planktonic assemblages. Statistically significant levels are indicated by asterisks as *($p < 0.05$), **($p < 0.01$) or ***($p < 0.001$).

the metacommunity, particularly under short HRTs.

In this study, the stochastic processes could play a role either by immigration of taxa (e.g., from the granules in the DSC to the FF biofilm), or dispersal (washout) of taxa (e.g., from granules and the FF biofilm), or undominated stochastic processes leading to random changes in community composition in the assemblages. Concurrently, deterministic processes could play a role due to inter-species interactions (e.g., syntrophic interactions), or environmental variables (e.g., LCFA concentrations, HRT). While the relative contribution of each process has remained controversial (Stegen et al., 2012), we found that deterministic and stochastic mechanisms had combined roles in the microbial community assembly, wherein, biofilm had the highest stochasticity among the assemblages (Fig. 4). The bioreactors were designed as retained-biomass systems in this study so as to minimize the washout of slow-growing species. Moreover, the biofilm compartment was designed to compensate for washout from the preceding sludge chamber (DSC). Microbes were washed upward from the variably performing DSC chamber (granules) to the FF chamber (biofilm), and onwards to the effluent. We hypothesize that within the metacommunity, fluctuating metabolite (substrate and intermediates) concentrations and microbial populations reached the biofilm from DSC, which resulted in a higher randomness in the biofilm than in the granules or effluent microbiomes.

As a variable selection accounted for the largest proportion (>50%) of the assembly processes, we considered it interesting to identify the environmental variables significantly linked to the variability in the observed communities. RDA with forward selection was employed (Vass et al., 2020), which showed that the stearate loading rate ($p < 0.001$), palmitate loading rate ($p < 0.01$), palmitate removal rate ($p < 0.05$) and caproate concentrations ($p < 0.01$) had a bearing on the variation in microbial community composition (Table 2). Specifically, this study could associate microbial community assembly with operational parameters (HRTs, and LCFA loading (stearate and palmitate)) (Table 2). These findings have transferrable implications to reactor operation strategies and could be employed to modulate microbial community assembly in anaerobic bioreactors operated at conditions similar to this study. For example, higher dispersal limitation was observed in granules than biofilms (Fig. 4), reflecting the utility of granulation in microbial retention under challenging operational conditions.

3.4. Environmental effects on microbial community dynamics

3.4.1. Environmental variables affecting microbial community composition and dynamics

Given that the microbial community diversity, composition, and assembly were differentiated in the assemblages and demonstrated predominant environmental filtering, we investigated the environmental variables that delineated the microbial community dynamics by applying correlation analysis. The concentrations of total and soluble COD, caproate (C_6), palmitate (C_{16}) and total LCFAs were strongly correlated ($p < 0.05$) to the taxa abundance (Fig. 5). The strength of association between the representative taxa and environmental variables was measured using Kendall correlation. Palmitate removal rate positively correlated to the representative taxa, *Geobacter*, *uncultured bacterium Syner-01*, *uncultured bacterium SJA-29* (family *Veillonellaceae*) and *Syntrophobacterales bacterium Delta 03*. Of these, *uncultured bacterium Syner-01*, and *uncultured bacterium SJA-29* (family *Veillonellaceae*) were negatively correlated to the concentrations of even-chained VFAs,

Table 2
Redundancy analysis (RDA) with forward selection using ADONIS to select the environmental variables most strongly associated with the variance of the observed communities.

Environmental variables	Df	SumsOfSqs	MeanSqs	F.Model	R^2	Pr(>F)	Significance
Stearate (C18:0) loading rate	1	0.6644	0.66441	6.1819	0.14982	0.0001	***
Methane yield (COD added)	1	0.3466	0.34657	3.2246	0.07815	0.0039	**
Caproate (C6) concentrations	1	0.3683	0.36828	3.4266	0.08305	0.004	**
Valerate (C5) concentrations	1	0.2945	0.29448	2.74	0.06641	0.0141	*
Palmitate (C16:0) loading rate	1	0.3405	0.34051	3.1683	0.07679	0.0046	**
Palmitate (C16:0) removal rate	1	0.2708	0.27084	2.52	0.06108	0.0201	*
Residuals	20	2.1495	0.10748	0.48471			
Total	26	4.4346	1				

Significance codes: 0 '***' 0.001 '**' 0.01 '*' 0.05 '.' 0.1 ' ' 1

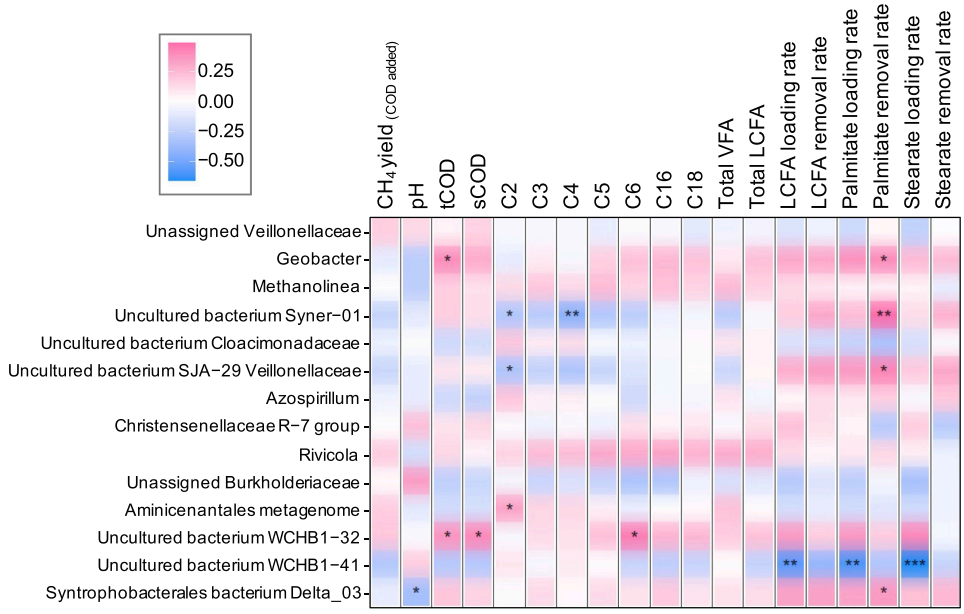

Fig. 5. The correlation heatmap of the representative taxa from granular (from DSC), biofilm (from FF) and planktonic (from effluent) assemblages with the environmental variables (metabolite concentrations and process performance parameters) prevailing in the different bioreactor compartments (DSC, FF, effluent). Kendall correlations between the representative taxa and the environmental variables were calculated. Significance levels are indicated by asterisks as *($p < 0.05$), **($p < 0.01$) or ***($p < 0.001$).

specifically acetate (C_2) or butyrate (C_4). Whilst the *uncultured bacterium WCHB1-32* (family *Prolixibacteraceae*) positively correlated to tCOD, sCOD and caproate (C_6) concentrations, the *uncultured bacterium* from order *WCHB1-41* (class *Kiritimatiellae*) negatively correlated with the loading rates of palmitate (C_{16}) and stearate (C_{18}), thereby delineating the roles of different fatty acids in structuring the dynamic non-core taxa in the assemblages.

3.4.2. *Anaerobic LCFA degradation by assemblages: Methanogenesis and syntrophic β-oxidation*

HRTs and LCFA loading rates influenced the representative taxa driving community dynamics in the granular, biofilm and planktonic assemblages (Fig. 5, Table 1). With decreasing HRTs and LCFA loading, equivalently increasing active populations of fermenters, β-oxidizers, and hydrogenotrophic and acetoclastic methanogens were required for degradation of the LCFAs at 20 °C. Methanogenesis is a conserved function mediated through methylotrophic, acetoclastic or hydrogenotrophic pathways. Among the archaeal taxa found in the granular sludge microbiome in this study, *Methanosaeta* was the only acetoclastic genus, and had the highest relative abundances as well as high prevalence in core microbiomes (Fig. 2,3). Earlier, *Methanosaeta* was found in high relative abundances in LCFA-degrading anaerobic consortia in both batch assays and continuous high-rate reactors at low temperatures (Paulo et al., 2020; Singh et al., 2019a, 2019b). In the current study, by analyzing 16S rRNA (cDNA) we could demonstrate the persistence and active role of *Methanosaeta* in granules and biofilm in the acetoclastic methanogenesis at 20 °C even at low HRTs and high LCFA loading. The retention times of cells within the granules and the biofilm are much longer than the applied HRTs, and presumably enabled maintainenance of slow-growing acetoclastic methanogens.

β-oxidation of LCFAs is a narrowly conserved function, wherein only few known species belonging to the genera *Syntrophus* (family *Syntrophaceae,* class *Deltaproteobacteria); Syntrophomonas,* and *Thermosyntropha* (family *Syntrophomonadaceae,* class *Clostridia*), and uncultured taxa (family *Clostridiaceae*, class *Clostridia*) (Baserba et al., 2012; Sousa et al., 2009). Thus, an examination of taxa belonging to the families *Syntrophomonadaceae* (class *Clostridia*) and *Syntrophaceae* (class *Deltaproteobacteria*) in this study was considered of interest to find taxa responsible for LCFA degradation. In our study, the relative abundance of genus *Syntrophomonas* was low (<0.5%), whereas taxa assigned to the family *Syntrophaceae* were highly abundant, consisting of *Syntrophus* and an uncultured *Syntrophaceae* taxon (Fig. 2). In previous studies, *Syntrophomonadaceae*-related taxa have been reported frequently from mesophilic or thermophilic anaerobic bioreactors treating fats, oils and grease (FOG)-rich wastes at relative abundances, that is, at 0.2–25% in sludges treating lipid-rich wastes (Hansen et al., 1999; Menes and Travers, 2006; Ziels et al., 2017). Concurrently, *Syntrophus*-affiliated taxa have been reported from diverse environments, including not only the mesophilic and thermophilic digesters treating palm-oil mill effluent (POME) and LCFAs (Hatamoto et al., 2007; Yoochatchaval et al., 2011), and mesophilic reactors treating cafeteria wastewater (Fujihira et al., 2018); but also the psychrophilic digesters treating food waste (Choudhary et al., 2020) and LCFA-rich wastewater (Singh et al., 2019a), low-temperature reactors treating LCFA-rich wastewater (Singh et al., 2019b), and psychrophilic digesters degrading stearate and alkanes (Grabowski et al., 2005). Meanwhile, abundant populations of both *Syntrophus* and *Syntrophomonas* have also been reported, e.g., from batch incubations digesting lipid-rich scum at 30 °C wherein the relative abundances increased for *Syntrophus* (3-fold) as well as *Syntrophomonas* (1.1-fold) (Fujihira et al., 2018). Thus, linking the prevalence of the β-oxidizing genera to the operational conditions has been confounding based on substrate (FOG, LCFA) and operational conditions (temperature, HRTs).

In our study, uncultured *Syntrophaceae* was the only putative β-oxidizer present at high relative abundances (Fig. 2) as well as in the core microbiomes (Fig. 3). Hence, an active role for *Syntrophaceae*-affiliated taxa (*Syntrophus* and uncultured) is implied in treating LCFA-rich wastewaters at low HRTs at 20 °C; supported by their psychrotolerant growth in granules as well as in biofilms (Fig. 2,3). Syntrophs are fastidious and despite playing a crucial role in global carbon cycling, their characterization has remained relatively obscure (Narihiro and Kamagata, 2017). Although taxonomic resolution of uncultured syntrophic bacteria below family level may still be challenging despite the use of high-end molecular methods (Hatamoto et al., 2007), we show that the use of new bioinformatics (i.e. data analytics) approaches offers alternative ways to link process performance with population dynamics in microbial communities. This may provide useful insights when low

microbial growth rates, or an abundance of uncultured taxa, confound analyses using conventional molecular approaches. The large proportion of unassigned and uncultured taxa in our study suggests that novel uncultured microbes may have a role in methanization of LCFAs in the granular and biofilm assemblages at low ambient temperatures. Future advancements should leverage genome-centric tools to connect the abundance of β-oxidizing bacteria to LCFA metabolism in response to diverse external stimuli, while simultaneously comprehending the functional expressions of *Syntrophus* and *Syntrophomonas* under those stimulus (James et al., 2019; Treu et al., 2016).

4. Conclusions

Multiple null modelling approaches systematically confirmed that combined deterministic and stochastic mechanisms influenced the microbial community assembly in high-rate bioreactors treating LCFA-rich wastewater at 20 °C. Variable selection (deterministic) accounted for the largest proportion (>50%) of the assembly processes, while undominated processes (26–36%) constituted the most important stochastic process. Abundant *Methanosaeta* and *Syntrophaceae* (*Syntrophus* and uncultured taxa) were prevalent in the core microbiomes, suggesting these taxa were critical in syntrophic LCFA-degradation. This study expands our understanding of the microbial community dynamics and assembly in complex metacommunities comprising granular, biofilm and planktonic assemblages mediating dairy waste bioconversion in innovative DSC-FF bioreactors.

CRediT authorship contribution statement

Suniti Singh: Conceptualization, Investigation, Data curation, Formal analysis, Writing – original draft, Writing – review & editing. **Johanna M. Rinta-Kanto:** Writing – review & editing. **Piet N.L. Lens:** Funding acquisition, Writing – review & editing. **Marika Kokko:** Writing – original draft, Writing – review & editing. **Jukka Rintala:** Funding acquisition, Writing – review & editing. **Vincent O'Flaherty:** Conceptualization, Supervision, Writing – review & editing. **Umer Zeeshan Ijaz:** Formal analysis, Supervision, Writing – review & editing. **: . Gavin Collins:** Funding acquisition, Conceptualization, Supervision, Writing – original draft, Writing – review & editing.

Declaration of Competing Interest

The authors declare they have no conflicts of interest.

Acknowledgements

This project has received funding from the European Union's Horizon 2020 research and innovation programme under the Marie Sklodowska-Curie European Joint Doctorate (EJD) in Advanced Biological Waste-To-Energy Technologies (ABWET), under grant agreement No 643071. VOF was supported by the Enterprise Ireland Technology Centres Programme (TC/2014/0016) and Science Foundation Ireland (14/IA/2371 and 16/RC/3889). UZI is further supported by a NERC Independent Research Fellowship (NE/L011956/1) and EPSRC (EP/P029329/1 and EP/V030515/1). GC, and DNA sequencing, was supported by a Science Foundation Ireland Career Development Award (17/CDA/4658).

Data availability

The sequencing data from this study are available through the NCBI database under the project accession number accession PRJNA657615.

Appendix A. Supplementary data

Supplementary data to this article can be found online at https://doi.org/10.1016/j.biortech.2021.126098.

References

Abdelgadir, A., Chen, X., Liu, J., Xie, X., Zhang, J., Zhang, K., Wang, H., Liu, N., 2014. Characteristics, process parameters, and inner components of anaerobic bioreactors. Biomed Res. Int. doi:10.1155/2014/841573.

Aqeel, H., Weissbrodt, D.G., Cerruti, M., Wolfaardt, G.M., Wilén, B.-M., Liss, S.N., 2019. Drivers of bioaggregation from flocs to biofilms and granular sludge. Environ. Sci. Water Res. Technol. 5 (12), 2072–2089. https://doi.org/10.1039/C9EW00450E.

Astals, S., Batstone, D.J., Mata-Alvarez, J., Jensen, P.D., 2014. Identification of synergistic impacts during anaerobic co-digestion of organic wastes. Bioresour. Technol. 169, 421–427. https://doi.org/10.1016/j.biortech.2014.07.024.

Baserba, M.G., Angelidaki, I., Karakashev, D., 2012. Effect of continuous oleate addition on microbial communities involved in anaerobic digestion process. Bioresour. Technol. 106, 74–81. https://doi.org/10.1016/j.biortech.2011.12.020.

Bolyen, E., Rideout, J.R., Dillon, M.R., Bokulich, N.A., Abnet, C.C., Al-Ghalith, G.A., Alexander, H., Alm, E.J., Arumugam, M., Asnicar, F., Bai, Y., Bisanz, J.E., Bittinger, K., Brejnrod, A., Brislawn, C.J., Brown, C.T., Callahan, B.J., Caraballo-Rodríguez, A.M., Chase, J., Cope, E.K., Da Silva, R., Diener, C., Dorrestein, P.C., Douglas, G.M., Durall, D.M., Duvallet, C., Edwardson, C.F., Ernst, M., Estaki, M., Fouquier, J., Gauglitz, J.M., Gibbons, S.M., Gibson, D.L., Gonzalez, A., Gorlick, K., Guo, J., Hillmann, B., Holmes, S., Holste, H., Huttenhower, C., Huttley, G.A., Janssen, S., Jarmusch, A.K., Jiang, L., Kaehler, B.D., Kang, K.B., Keefe, C.R., Keim, P., Kelley, S.T., Knights, D., Koester, I., Kosciolek, T., Kreps, J., Langille, M.G.I., Lee, J., Ley, R., Liu, Y.-X., Loftfield, E., Lozupone, C., Maher, M., Marotz, C., Martin, B.D., McDonald, D., McIver, L.J., Melnik, A.V., Metcalf, J.L., Morgan, S.C., Morton, J.T., Naimey, A.T., Navas-Molina, J.A., Nothias, L.F., Orchanian, S.B., Pearson, T., Peoples, S.L., Petras, D., Preuss, M.L., Pruesse, E., Rasmussen, L.B., Rivers, A., Robeson, M.S., Rosenthal, P., Segata, N., Shaffer, M., Shiffer, A., Sinha, R., Song, S.J., Spear, J.R., Swafford, A.D., Thompson, L.R., Torres, P.J., Trinh, P., Tripathi, A., Turnbaugh, P.J., Ul-Hasan, S., van der Hooft, J.J.J., Vargas, F., Vázquez-Baeza, Y., Vogtmann, E., von Hippel, M., Walters, W., Wan, Y., Wang, M., Warren, J., Weber, K.C., Williamson, C.H.D., Willis, A.D., Xu, Z.Z., Zaneveld, J.R., Zhang, Y., Zhu, Q., Knight, R., Caporaso, J.G., 2019. Reproducible, interactive, scalable and extensible microbiome data science using QIIME 2. Nat. Biotechnol. 37 (8), 852–857. https://doi.org/10.1038/s41587-019-0209-9.

Braz, G.H.R., Fernandez-Gonzalez, N., Lema, J.M., Carballa, M., 2019. Organic overloading affects the microbial interactions during anaerobic digestion in sewage sludge reactors. Chemosphere 222, 323–332. https://doi.org/10.1016/j.chemosphere.2019.01.124.

Caporaso, J.G., Kuczynski, J., Stombaugh, J., Bittinger, K., Bushman, F.D., Costello, E.K., Fierer, N., Peña, A.G., Goodrich, J.K., Gordon, J.I., Huttley, G.A., Kelley, S.T., Knights, D., Koenig, J.E., Ley, R.E., Lozupone, C.A., McDonald, D., Muegge, B.D., Pirrung, M., Reeder, J., Sevinsky, J.R., Turnbaugh, P.J., Walters, W.A., Widmann, J., Yatsunenko, T., Zaneveld, J., Knight, R., 2010. QIIME allows analysis of high-throughput community sequencing data. Nat. Methods 7 (5), 335–336. https://doi.org/10.1038/nmeth.f.303.

Caporaso, J.G., Lauber, C.L., Walters, W.A., Berg-Lyons, D., Lozupone, C.A., Turnbaugh, P.J., Fierer, N., Knight, R., 2011. Global patterns of 16S rRNA diversity at a depth of millions of sequences per sample. Proc. Natl. Acad. Sci. 108 (Supplement_1), 4516–4522. https://doi.org/10.1073/pnas.1000080107.

Chen, Y., Wang, C., Dong, S., Jiang, L., Shi, Y., Li, X., Zou, W., Tan, Z., 2019. Microbial community assembly in detergent wastewater treatment bioreactors: Influent rather than inoculum source plays a more important role. Bioresour. Technol. 287, 121467. https://doi.org/10.1016/j.biortech.2019.121467.

Choudhary, A., Kumar, A., Govil, T., Sani, R.K., Gorky, Kumar, S., 2020. Sustainable production of biogas in large bioreactor under psychrophilic and mesophilic conditions. J. Environ. Eng. (United States) 146, 1–10. doi:10.1061/(ASCE)EE.1943-7870.0001645.

Ferguson, R.M.W., Coulon, F., Villa, R., 2018. Understanding microbial ecology can help improve biogas production in AD. Sci. Total Environ. 642, 754–763. https://doi.org/10.1016/j.scitotenv.2018.06.007.

Fujihira, T., Seo, S., Yamaguchi, T., Hatamoto, M., Tanikawa, D., 2018. High-rate anaerobic treatment system for solid/lipid-rich wastewater using anaerobic baffled reactor with scum recovery. Bioresour. Technol. 263, 145–152. https://doi.org/10.1016/j.biortech.2018.04.091.

Grabowski, Agnès, Blanchet, Denis, Jeanthon, Christian, 2005. Characterization of long-chain fatty-acid-degrading syntrophic associations from a biodegraded oil reservoir. Res. Microbiol. 156 (7), 814–821. https://doi.org/10.1016/j.resmic.2005.03.009.

Hansen, Kaare H., Ahring, Birgitte K., Raskin, Lutgarde, 1999. Quantification of syntrophic fatty acid-β-oxidizing bacteria in a mesophilic biogas reactor by oligonucleotide probe hybridization. Appl. Environ. Microbiol. 65 (11), 4767–4774.

Hatamoto, Masashi, Imachi, Hiroyuki, Yashiro, Yuto, Ohashi, Akiyoshi, Harada, Hideki, 2007. Diversity of anaerobic microorganisms involved in long-chain fatty acid degradation in methanogenic sludges as revealed by RNA-based stable isotope probing. Appl. Environ. Microbiol. 73 (13), 4119–4127. https://doi.org/10.1128/AEM.00362-07.

Heidrich, E.S., Dolfing, J., Wade, M.J., Sloan, W.T., Quince, C., Curtis, T.P., 2018. Temperature, inocula and substrate: Contrasting electroactive consortia, diversity and performance in microbial fuel cells. Bioelectrochemistry 119, 43–50. https://doi.org/10.1016/j.bioelechem.2017.07.006.

James, Kimberly L., Kung, Johannes W., Crable, Bryan R., Mouttaki, Housna, Sieber, Jessica R., Nguyen, Hong H., Yang, Yanan, Xie, Yongming, Erde, Jonathan, Wofford, Neil Q., Karr, Elizabeth A., Loo, Joseph A., Ogorzalek Loo, Rachel R.,

Gunsalus, Robert P., McInerney, Michael J., 2019. Syntrophus aciditrophicus uses the same enzymes in a reversible manner to degrade and synthesize aromatic and alicyclic acids. Environ. Microbiol. 21 (5), 1833–1846. https://doi.org/10.1111/emi.2019.21.issue-510.1111/1462-2920.14601.

Lahti, L., Shetty, S., Blake, T., Salojarvi, J., 2019. Tools for microbiome analysis in R. Microbiome package. Bioconductor. [WWW Document]. http://microbiome.github.io/microbiome.

Li, K., Yun, J., Zhang, H., Yu, Z., 2019. Full-scale anaerobic reactor samples would be more suitable than lab-scale anaerobic reactor and natural samples to inoculate the wheat straw batch anaerobic digesters. Bioresour. Technol. 293, 1–9. https://doi.org/10.1016/j.biortech.2019.122040.

Liébana, Raquel, Modin, Oskar, Persson, Frank, Szabó, Enikö, Hermansson, Malte, Wilén, Britt-Marie, 2019. Combined Deterministic and Stochastic Processes Control Microbial Succession in Replicate Granular Biofilm Reactors. Environ. Sci. Technol. 53 (9), 4912–4921. https://doi.org/10.1021/acs.est.8b0666910.1021/acs.est.8b06669.s00110.1021/acs.est.8b06669.s002.

Lucas, R., Kuchenbuch, A., Fetzer, I., Harms, H., Kleinsteuber, S., 2015. Long-term monitoring reveals stable and remarkably similar microbial communities in parallel full-scale biogas reactors digesting energy crops. FEMS Microbiol. Ecol. 91, 1–11. https://doi.org/10.1093/femsec/fiv004.

McCarty, Nicholas S., Ledesma-Amaro, Rodrigo, 2019. Synthetic Biology Tools to Engineer Microbial Communities for Biotechnology. Trends Biotechnol. 37 (2), 181–197. https://doi.org/10.1016/j.tibtech.2018.11.002.

Menes, R.J., Travers, D., 2006. Detection of fatty acid beta-oxidizing syntrophic bacteria by fluorescence in situ hybridization. Water Sci. Technol. 54, 33–39. https://doi.org/10.2166/wst.2006.483.

Narihiro, Takashi, Kamagata, Yoichi, 2017. Genomics and metagenomics in microbial ecology: Recent advances and challenges. Microbes Environ. 32 (1), 1–4. https://doi.org/10.1264/jsme2.ME3201rh.

Nemergut, Diana R., Schmidt, Steven K., Fukami, Tadashi, O'Neill, Sean P., Bilinski, Teresa M., Stanish, Lee F., Knelman, Joseph E., Darcy, John L., Lynch, Ryan C., Wickey, Phillip, Ferrenberg, Scott, 2013. Patterns and Processes of Microbial Community Assembly. Microbiol. Mol. Biol. Rev. 77 (3), 342–356. https://doi.org/10.1128/MMBR.00051-12.

Nikolaeva, S., Sanchez, E., Borja, R., 2013. Dairy wastewater treatment by anaerobic fixed bed reactors from laboratory to pilot-scale plant :a case study in Costa Rica operating at ambient temperature. Int. J. Environ. Res. 7, 759–766.

Nikolova, C., Ijaz, U.Z., Gutierrez, T., 2021. Exploration of marine bacterioplankton community assembly mechanisms during chemical dispersant and surfactant-assisted oil biodegradation. Ecol. Evol. 1–13 https://doi.org/10.1002/ece3.8091.

Ning, Daliang, Deng, Ye, Tiedje, James M., Zhou, Jizhong, 2019. A general framework for quantitatively assessing ecological stochasticity. Proc. Natl. Acad. Sci. U. S. A. 116 (34), 16892–16898. https://doi.org/10.1073/pnas.1904623116.

Paulo, Lara M., Castilla-Archilla, Juan, Ramiro-Garcia, Javier, Escamez-Picón, José Antonio, Hughes, Dermot, Mahony, Thérèse, Murray, Michael, Wilmes, Paul, O'Flaherty, Vincent, 2020. Microbial Community Redundancy and Resilience Underpins High-Rate Anaerobic Treatment of Dairy-Processing Wastewater at Ambient Temperatures. Front. Bioeng. Biotechnol. 8 https://doi.org/10.3389/fbioe.2020.0019210.3389/fbioe.2020.00192.s00110.3389/fbioe.2020.00192.s00210.3389/fbioe.2020.00192.s00310.3389/fbioe.2020.00192.s00410.3389/fbioe.2020.00192.s00510.3389/fbioe.2020.00192.s006.

Petropoulos, Evangelos, Yu, Yongjie, Tabraiz, Shamas, Yakubu, Aminu, Curtis, Thomas P., Dolfing, Jan, 2019. High rate domestic wastewater treatment at 15°C using anaerobic reactors inoculated with cold-adapted sediments/soils-shaping robust methanogenic communities. Environ. Sci. Water Res. Technol. 5 (1), 70–82. https://doi.org/10.1039/C8EW00410B.

Pommerville, J.C., 2014. Fundamentals of Microbiology, Burlington, MA: Jones & Bartlett Learning. doi:10.1017/CBO9781107415324.004.

Singh, S., 2019. High rate anaerobic treatment of LCFA-containing wastewater at low temperature. PhD Diss. Tampere Univ, Tampere, Finland.

Singh, S., Holohan, B.C., Mills, S., Castilla-Archilla, J., Kokko, M., Rintala, J., Lens, P.N. L., Collins, G., O'Flaherty, V., 2020. Enhanced methanization of long chain fatty acid wastewater at 20°C in the novel dynamic sludge chamber-fixed film bioreactor. Front. Energy Res. 8, 1–13. https://doi.org/10.3389/fenrg.2020.00166.

Singh, S., Rinta-Kanto, J.M., Kettunen, R., Lens, P., Collins, G., Kokko, M., Rintala, J., 2019a. Acetotrophic activity facilitates methanogenesis from LCFA at low temperatures: screening from mesophilic inocula. Archaea 2019, 1–16. https://doi.org/10.1155/2019/1751783.

Singh, S., Rinta-Kanto, J.M., Kettunen, R., Tolvanen, H., Lens, P., Collins, G., Kokko, M., Rintala, J., 2019b. Anaerobic treatment of LCFA-containing synthetic dairy wastewater at 20 °C: Process performance and microbial community dynamics. Sci. Total Environ. 691, 960–968. https://doi.org/10.1016/j.scitotenv.2019.07.136.

Sousa, D.Z., Smidt, H., Alves, M.M., Stams, A.J.M., 2009. Ecophysiology of syntrophic communities that degrade saturated and unsaturated long-chain fatty acids. FEMS Microbiol. Ecol. 68, 257–272. https://doi.org/10.1111/j.1574-6941.2009.00680.x.

Stegen, J.C., Lin, X., Fredrickson, J.K., Konopka, A.E., 2015. Estimating and mapping ecological processes influencing microbial community assembly. Front. Microbiol. 6, 1–15. https://doi.org/10.3389/fmicb.2015.00370.

Stegen, James C, Lin, Xueju, Konopka, Allan E, Fredrickson, James K, 2012. Stochastic and deterministic assembly processes in subsurface microbial communities. ISME J. 6 (9), 1653–1664. https://doi.org/10.1038/ismej.2012.22.

Trego, A.C., McAteer, P.G., Nzeteu, C., Mahony, T., Abram, F., Ijaz, U.Z., O'Flaherty, V., 2021. Combined Stochastic and Deterministic Processes Drive Community Assembly of Anaerobic Microbiomes During Granule Flotation. Front. Microbiol. 12, 1–14. https://doi.org/10.3389/fmicb.2021.666584.

Treu, L., Kougias, P.G., Campanaro, S., Bassani, I., Angelidaki, I., 2016. Deeper insight into the structure of the anaerobic digestion microbial community; The biogas microbiome database is expanded with 157 new genomes. Bioresour. Technol. 216, 260–266. https://doi.org/10.1016/j.biortech.2016.05.081.

Vanwonterghem, Inka, Jensen, Paul D, Dennis, Paul G, Hugenholtz, Philip, Rabaey, Korneel, Tyson, Gene W, 2014. Deterministic processes guide long-term synchronised population dynamics in replicate anaerobic digesters. ISME J. 8 (10), 2015–2028. https://doi.org/10.1038/ismej.2014.50.

Vass, M., Székely, A.J., Lindström, E.S., Langenheder, S., 2020. Using null models to compare bacterial and microeukaryotic metacommunity assembly under shifting environmental conditions. Sci. Rep. 10, 1–13. https://doi.org/10.1038/s41598-020-59182-1.

Vellend, Mark, 2010. Conceptual Synthesis in Community Ecology. Q. Rev. Biol. 85 (2), 183–206.

Wang, Jianjun, Shen, Ji, Wu, Yucheng, Tu, Chen, Soininen, Janne, Stegen, James C, He, Jizheng, Liu, Xingqi, Zhang, Lu, Zhang, Enlou, 2013. Phylogenetic beta diversity in bacterial assemblages across ecosystems: Deterministic versus stochastic processes. ISME J. 7 (7), 1310–1321. https://doi.org/10.1038/ismej.2013.30.

Xu, R., Yu, Z., Zhang, S., Meng, F., 2019. Bacterial assembly in the bio-cake of membrane bioreactors: Stochastic vs. deterministic processes. Water Res. 157, 535–545. https://doi.org/10.1016/j.watres.2019.03.093.

Xu, Ronghua, Zhang, Shaoqing, Meng, Fangang, 2020. Large-sized planktonic bioaggregates possess high biofilm formation potentials: Bacterial succession and assembly in the biofilm metacommunity. Water Res. 170, 115307. https://doi.org/10.1016/j.watres.2019.115307.

Yoochatchaval, W., Kumakura, S., Tanikawa, D., Yamaguchi, T., Yunus, M.F.M., Chen, S. S., Kubota, K., Harada, H., Syutsubo, K., 2011. Anaerobic degradation of palm oil mill effluent (POME). Water Sci. Technol. 64, 2001–2008. https://doi.org/10.2166/wst.2011.782.

Yuan, H., Mei, R., Liao, J., Liu, W.-T., 2019. Nexus of Stochastic and Deterministic Processes on Microbial Community Assembly in Biological Systems. Front. Microbiol. 10, 1–12. https://doi.org/10.3389/fmicb.2019.01536.

Zhou, J., 2017. Stochastic community assembly : does it matter in microbial ecology. Microbiol. Mol. Biol. Rev. 81, 1–32.

Ziels, R.M., Beck, D.A.C., Stensel, H.D., 2017. Long-chain fatty acid feeding frequency in anaerobic codigestion impacts syntrophic community structure and biokinetics. Water Res. 117, 218–229. https://doi.org/10.1016/j.watres.2017.03.060.